

and the homotropylium ion VI. The only guide is a comparison with the solution spectra. While too few cases have been studied for reliable generalization, the solution and gas-phase spectra of several protonated aromatics have been found to be closely similar,^{4,11} with the gas-phase photodissociation peaks showing a blue shift of zero to 1000 cm^{-1} , and (in one case⁴) similar cross section.

Assuming methyltropylium ion to be spectroscopically similar to tropylium ion, structure V can be ruled out at once, as the longest wavelength tropylium ion peak is at 36 560 cm^{-1} .¹² The choice between IV and VI is quite clear: VI has solution peaks at 43 010 ($\sigma = 1.3 \times 10^{-16} \text{ cm}^2$) and 32 100 cm^{-1} ($\sigma = 1.2 \times 10^{-17} \text{ cm}^2$); IV is not known in solution, but by analogy with its alkyl-substituted analogues¹² can be presumed to have peaks at about 31 250 ($\sigma \approx 4 \times 10^{-17} \text{ cm}^2$) and 25 600 cm^{-1} ($\sigma \approx 4 \times 10^{-18} \text{ cm}^2$). Both in peak positions and (to an order of magnitude) in cross sections the photodissociation spectrum matches the spectrum expected for styryl ion, IV, and we conclude that this is the ultimate product of gas-phase H_3O^+ protonation of all three of the C_8H_8 isomers studied.

H_3O^+ is a rather energetic protonating reagent, making available about 30 kcal of excess energy to protonated styrene (thermochemical values for COT and barrelene are not available). Wide traversal of the C_8H_9^+ potential surface is thus not very surprising. A detailed study of this question with other protonating agents is in progress; however, protonation of COT by proton transfer from tetrahydrofuran gives an ion apparently identical with that obtained from H_3O^+ protonation.¹⁴ THF is a much milder protonating agent, being 26 kcal more basic than water and only 4 kcal less basic than styrene,¹⁵ so that even with much lower internal energy rearrangement still occurs in the C_8H_9^+ ions.

Conclusion

The results of this study are in accord with the limited picture thus far built up of gas-phase hydrocarbon rearrangements: the radical cations formed by electron bombardment of the three C_8H_8 isomers do not rearrange to a common structure, and at least styrene and barrelene ions appear to

retain the structure of the parent neutral. The ions formed by H_3O^+ protonation of the isomers, however, undergo complete rearrangement to structure IV within the time scale of seconds appropriate to this technique, indicating that IV is the most stable gas-phase C_8H_9^+ structure.

Acknowledgment is made to the donors of the Petroleum Research Fund, administered by the American Chemical Society, to the National Science Foundation, and to the U.S. Air Force Geophysical Laboratory for support of this research. We are indebted to Professor Leo Paquette for his generous provision of the barrelene sample.

References and Notes

- (1) (a) Case Western Reserve University; (b) University of Southern California.
- (2) (a) See, for instance, R. C. Dunbar, *Anal. Chem.*, **48**, 723 (1976). (b) E. W. Fu and R. C. Dunbar, *J. Am. Chem. Soc.*, **100**, 2283 (1978); E. W. Fu, Ph.D. Thesis, Case Western Reserve University, 1976.
- (3) We are grateful to Professor Leo Paquette for kindly providing the sample.
- (4) R. C. Dunbar, E. W. Fu, and G. A. Olah, *J. Am. Chem. Soc.*, **99**, 7502 (1977).
- (5) E. W. Fu, P. P. Dymerski, and R. C. Dunbar, *J. Am. Chem. Soc.*, **98**, 337 (1976).
- (6) One of the important problems with the steady-state operating conditions of ref 2b is the possibility that a nonreactive ion species accumulates in the ion trap to an abundance far greater than its true relative abundance, as apparently occurred with a C_8H_8^+ isomer in the COT experiments. Such problems are eliminated or at least greatly reduced in pulsed operation.
- (7) C. Batich, P. Bischof, and E. Heilbronner, *J. Electron Spectrosc. Relat. Phenom.*, **1**, 333 (1972-1973).
- (8) E. Haselbach, E. Heilbronner, and G. Schröder, *Helv. Chim. Acta*, **54**, 153 (1971).
- (9) (a) R. C. Dunbar, *Chem. Phys. Lett.*, **32**, 508 (1975); (b) R. C. Dunbar and H. H. Teng, *J. Am. Chem. Soc.*, **100**, 2279 (1978).
- (10) Attempts to check the homogeneity of the barrelene ion population at 366 and 580 nm were inconclusive, and the possibility of a mixed ion population cannot be ruled out. It can only be said that none of the peaks in this spectrum corresponds to any peak of other known C_8H_8 spectra, except that a small extent of rearrangement to the COT^+ structure cannot be ruled out, as is seen from Figure 1.
- (11) B. S. Freiser and J. L. Beauchamp, *J. Am. Chem. Soc.*, **98**, 265, 3136 (1976).
- (12) S. Winstein in "Carbonium Ions", Vol. 1, G. A. Olah and P. v. R. Schleyer, Ed., Wiley-Interscience, New York, N.Y., 1968, p 981.
- (13) G. A. Olah, C. U. Pittman, and M. C. R. Symons in ref 12, p 186.
- (14) E. W. Fu and R. C. Dunbar, to be published.
- (15) J. F. Wolf, R. H. Staley, I. Koppel, M. Taagepara, R. T. McIver, Jr., J. L. Beauchamp, and R. W. Taft, *J. Am. Chem. Soc.*, **99**, 5417 (1977).

A MINDO/3 Study of the Bridged Pyramidal C_8H_9 Cation and Its Congeners

Charles W. Jefford,* Jiri Mareda, Jean-Claude Perlberger, and Ulrich Burger*

Contribution from the Department of Organic Chemistry, University of Geneva, 1211 Geneva 4, Switzerland. Received July 11, 1978

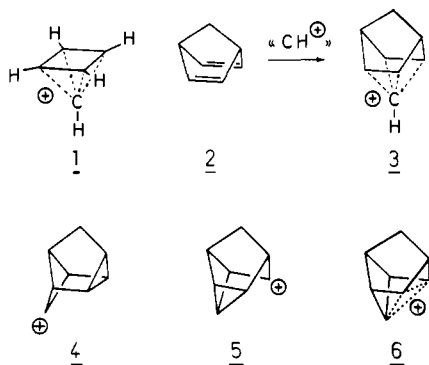
Abstract: The heats of formation, geometries, and formal atomic charges have been calculated for the bridged bishomo pyramidal C_8H_9 cation together with 13 of its congeners. Minimum energy reaction paths have been determined interconnecting the pyramidal cation with its valence isomers.

Introduction

Some time ago the ingenious suggestion was made that the most stable member of the C_5H_5^+ family of cations is the square pyramidal species **1**. Although subsequent calculations¹⁻⁴ have considerably refined the original proposal,⁵ it has nonetheless given rise to the innovatory principle that stable, pyramidal cations may be created by the formal centrolinear

addition of the carbyne cation to cyclic polyenes containing $4n$ π electrons.⁶ A pertinent illustration is the bridged bis homologue **3** obtained by formal adjunction of the carbyne cation to the endo side of norbornadiene (**2**), a classic example of a bishomo-conjugated diene.⁷

NMR spectroscopic evidence has been presented in favor of **3**,⁸ however, it is not unambiguous as it could well be compatible with rapid equilibration between classical cations such



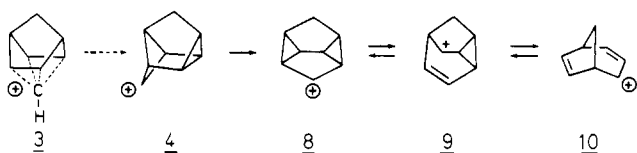
as **4** and **5** and their mirror image forms. A more subtle alternative is that the spectrum might be due to fast degenerate automerization of the trishomocyclopropenyl cation **6**.⁸⁻¹⁰

Clearly, here is a case where an appropriate quantum mechanical calculation could resolve this apparent dilemma by revealing the physical properties and relative stabilities of the contending cations. Moreover, information could be obtained on the behavior of **3** and closely related carbocations. Although several experimental studies have been performed on **3** and its congeners, interpretations of the results remain incomplete. On the other hand, calculation would be equally revealing on experimentally inaccessible species.

The procedure for calculation should fulfill two conditions. Firstly, it should have been tested for as many structures as possible so that the properties of uncharged molecules as well as carbocations can be accurately predicted. Secondly, since many of the ions are nonclassical, it should be able to minimize their total energy without making any assumptions about their geometry. Consequently, the procedure we have used is the MINDO/3 semiempirical SCF MO method.¹¹ It has already been adequately tested for many neutral molecules, as well as classical and nonclassical carbocations, not only for calculating molecular properties, but also for charting the course of reactions.¹²

The quantities of interest, which have been calculated, are the heats of formation (ΔH_f), the molecular geometries, and the formal atomic charges.^{13,14} In addition, the minimum energy reaction paths (MERP) connecting the pyramidal cation **3** to its classical isomers by haptotropic¹⁵ and sigmatropic transformations have been computed. All the present calculations were carried out using the standard MINDO/3 program with the associated DFP geometry procedure.¹¹ The best geometries of individual cations were sought by minimizing the energy with respect to all geometrical variables without any assumption being made. However, when we examined the bending of the apical methine carbon atom of **3** away from the molecular C₂ axis, it became necessary for reasons of computational economy to impose coplanarity on the four basal carbon atoms (vide infra). Clearly, such a restriction may well have resulted in the fortuitous selection of a particular reaction pathway over energetically more favorable alternatives. Nevertheless, the remarkable concordance of our results with the experimental facts is a good sign that our assumption was correct. Apart from this haptotropic reorganization, the cations selected (**4**–**15**) are related by simple sequences of 1,2 (or 1,3) carbon shifts of varying probability. The energies of all the relevant sigmatropic shifts could be conveniently calculated by the simple expedient of

Scheme 1

Table I. Calculated Heats of Formation (ΔH_f) of Selected C₈H₉ Carbocations

Ion no.	ΔH_f kcal/mol	Ion no.	ΔH_f kcal/mol
<u>3</u>	272.92	<u>10</u>	243.36
<u>4</u>	263.91	<u>11</u>	260.41
<u>5</u>	289.62	<u>12</u>	246.46
<u>6</u>	275.68	<u>13</u>	229.22
<u>7</u>	286.47	<u>14</u>	228.17
<u>8</u>	242.91	<u>15</u>	non-stable transient species
<u>9</u>	245.81	<u>16</u>	non-stable transient species

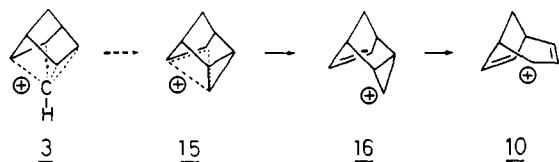
varying the particular carbon-carbon distance. Nearly all the cations or their polymethyl derivatives^{9,16} which we have considered correspond to real chemical entities which intervene in reactions, such as the thermal decomposition of diazonium ions,^{8,10} the solvolyses of tosylates^{17,18} and triflates,¹⁹ and the ionization of appropriate substrates in superacid media.^{8,20}

Results and Discussion

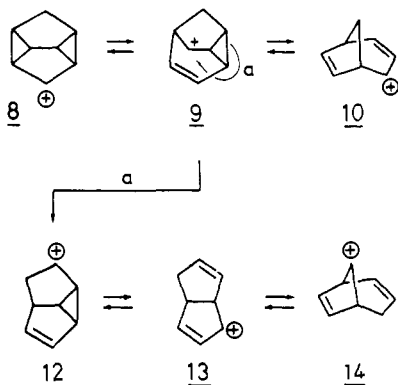
Heats of Formation. Inspection of the heats of formation (Table I) reveals that the pyramidal cation **3** is one of the less stable members of the family of C₈H₉⁺ ions, displaying a significant difference of some 43–45 kcal/mol compared with the most stable cations of the series, viz., the allylic and homoallylic cations **13** and **14**. If the cyclobutyl cation **4** is taken as the point of departure, then the relative values of the heats of formation indicate that there is little propensity for **4** to adopt the pyramidal structure **3**. The inverse process, namely, the haptotropic opening of **3** to **4**, appears attractive. On the other hand, the secondary cation **5** possesses an even greater heat of formation than **3**. Accordingly, the purported NMR spectrum⁸ of **3** is scarcely likely to be due to the dynamic average of a rapidly equilibrating mixture of **4** and **5**.

Cation **4** can be ruled out as the spectral species on account of its tendency to collapse by Wagner-Meerwein shift to the bicyclopopylcarbanyl cation **8**. In its turn, **8** can convert itself easily to the energetically similar species **9** and **10** by a simple series of shifts (Scheme I).

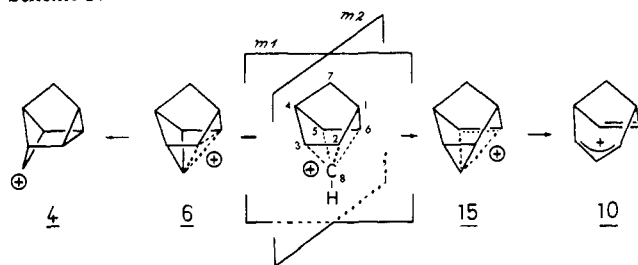
Scheme II



Scheme III



Scheme IV



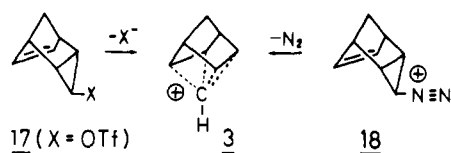
If we now look for other candidates among the $C_8H_9^+$ cations that might be easily accessible from **3** by a simple one-step transformation, the allylic ion **10** is an obvious choice. Unfortunately, the nonstable transient species **15** and **16** intervene and constitute a prohibitively high energy barrier (Scheme II).

The remaining cations (**11–14**), comprising the most stable species in our series, differ too much in their skeletons from **3** to be plausible one-step neighbors of the latter on the potential energy surface. Although the energetically similar species **13** and **14** are interrelated by simple shifts, their formation from the group of ions **8**, **9**, and **10** presents difficulty. A one-step rearrangement of **9** to produce **12**, although valid for the permethylated analogues,¹⁶ is quite unlikely here, as its activation barrier is calculated to be some 26.5 kcal/mol²³ (Scheme III). Accordingly, it comes as no surprise that leakage between the two groups of ions **8**, **9**, **10** and **12**, **13**, **14** is not observed under solvolysis conditions.^{21,18}

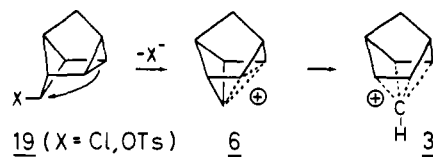
After this prospection of the $C_8H_9^+$ system, based on heats of formation, we now turn our attention to the energy surface immediately surrounding the pyramidal species **3**. There are two important questions. How high are the barriers which separate **3** from its haptotropic isomers (**4** and **10**), and what is the role of the homocyclopropenyl species **6** and **15** in these isomerizations?

Minimum Energy Reaction Paths (MERP). In order to probe the energy surface in the vicinity of **3**, the apical carbon atom of the pyramidal species needs to be bent away from the C_2 axis. There are two ways of doing this. The C_8 atom can be displaced progressively either in the plane bisecting the bridgehead carbons (m_1) to ultimately give **4** after passing through the species **6**, or moved in the plane (m_2) orthogonal to the first to generate **10** after passing through **15** (Scheme IV). In both cases, the four basal carbon atoms (C_2 , C_3 , C_5 , and C_6) are kept coplanar. As mentioned previously, for the

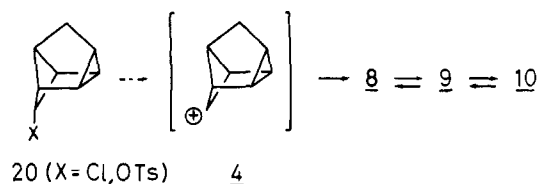
Scheme V



Scheme VI



Scheme VII



subsequent cationic rearrangements, i.e., $4 \rightarrow 8$, $8 \rightarrow 9$, and $9 \rightarrow 10$, the carbon-carbon distances of the bonds to be broken are designated as the reaction coordinates without imposing any geometric restrictions.

The results, namely, the connectivity and the magnitude of the barriers between the cations, are most revealing (Figure 1). First of all, it is seen that the pyramidal cation **3** corresponds to a local minimum. On its right it is protected by a considerable energy barrier (A) of some 35.8 kcal/mol represented by a nonstable transient species, the endo cyclopropyl cation **16**. Close by lies its near relative, the delocalized structure **15**. Obviously, there is little chance that **3** will rearrange to cation **10** by making the direct ascent over the top of A. On the other hand, kinetic entry to **3** from the side of A should be eminently feasible. Accordingly, it is to be expected that ionization of suitable *endo-anti*-tricyclo[3.2.1.0^{2,4}]octen-6-yl-3 derivatives (**17**) would give **15** and shortly thereafter **3**. Appropriately enough, the solvolysis of the triflate **17** ($X = OTf$)¹⁹ and the thermal decay of the corresponding diazonium ion (**18**)^{8,10} give products which are best explained in terms of the intermediate cation **3** (Scheme V).

Under nonquenching conditions, for example, in superacid medium, cation **3** is effectively prevented from spontaneous collapse enabling it to be observed by NMR spectroscopy⁸ thanks to the existence of a smaller, but still effective, energy barrier of 12.24 kcal/mol (B). Very close to **3** lies the trishomocyclopropenyl cation **6**.²² The computed difference in heats of formation (2.8 kcal/mol) and the negligible barrier (0.2 kcal/mol) separating **6** from **3** are too small to permit a distinction between these ions. Formation of cation **3** should also be feasible from the side of barrier B. Thus, heterolyses of suitable derivatives (**19**) having *exo*-disposed leaving groups should afford **3** via **6**. The generation of **3** in superacid medium from chloride **19** ($X = Cl$) is a good illustration. Expulsion of the *exo*-disposed leaving group aided by participation of the cyclopropane ring generates the transient species **6**. A slight skeletal adjustment produces **3**. Furthermore, the acetolysis of the corresponding tosylate **19** ($X = OTs$) can also be nicely interpreted by the intermediacy of **3**¹⁷ (Scheme VI). On the other hand, it is predicted from the MERP diagram (Figure 1) that heterolysis of the *endo* epimers (**20**) will not produce the pyramidal species **3** as the energy surface would be entered on the left-hand side of barrier B. As a result, products deriving from **4**, or more likely, from **8**, **9**, and **10**, are to be expected instead (Scheme VII).

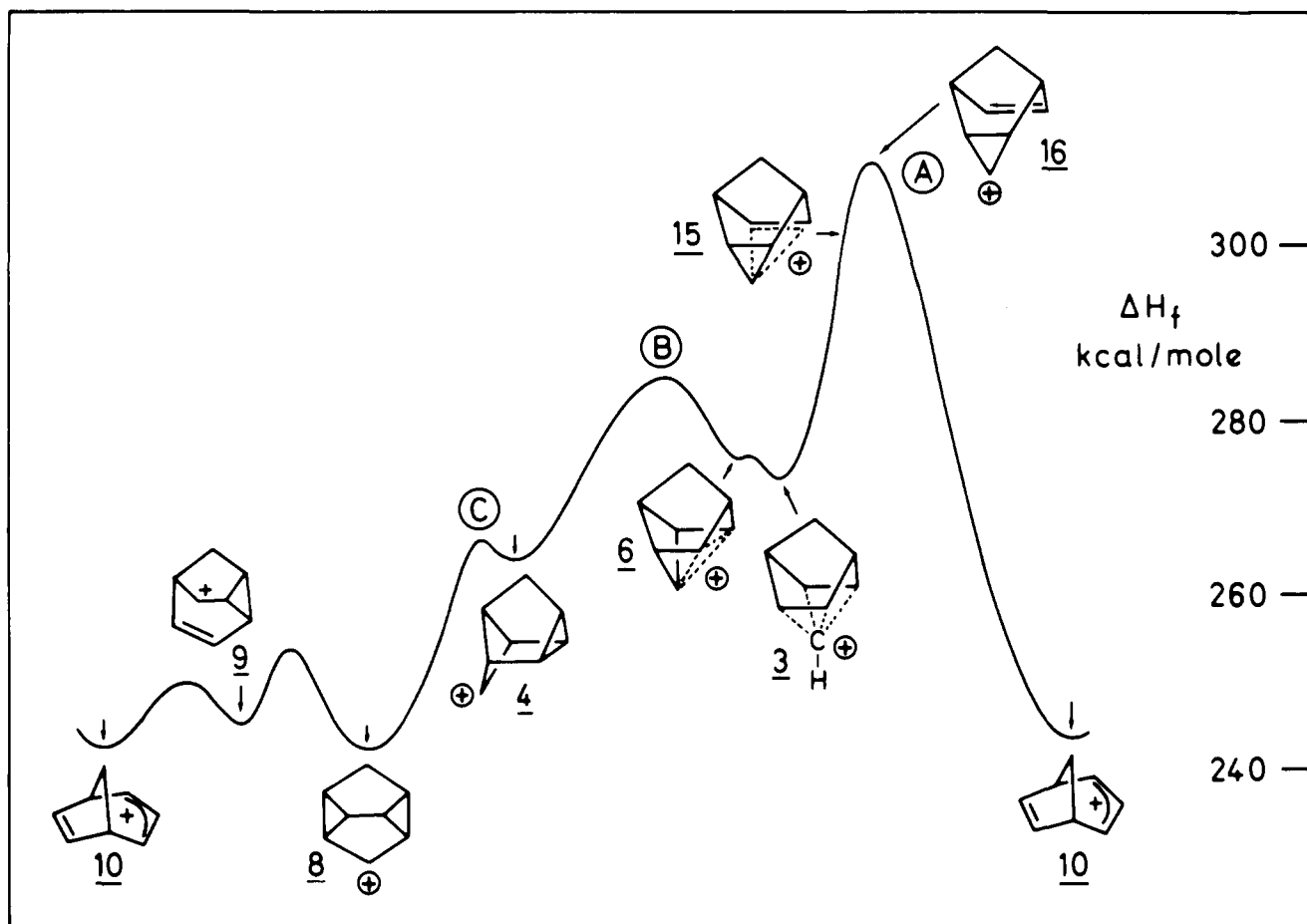


Figure 1.

This now brings us to the crucial question concerning the nature of the cyclobutyl cation **4**. According to our MINDO/3 calculations, this species is a discrete intermediate, barely prevented from undergoing a 1,2 shift ($4 \rightarrow 8$) by a tiny energy barrier C (1.9 kcal/mol). Again, such a barrier has little chemical meaning. Most probably, the ionization of **20** will be coupled energetically to the Wagner–Meerwein rearrangement ($4 \rightarrow 8$), which means that the solvolyses of **20** will be anchimerically assisted. It is perhaps significant that the preparation of tosylate **20** ($X = OTs$) has yet to be reported. Similarly, the chloride **20** ($X = Cl$) dissociates far more readily than its epimer **19** ($X = Cl$).²³

Structural Details. The present calculations also provide some unexpected insights into the physical and chemical properties of the pyramidal cation and its isomers. Firstly, the overall shape of **3** turns out to be very similar to those calculated^{25,3} by MINDO/2 and MINDO/3 for the unbridged bishomo cation **21** and the parent cation **1** (Figure 2). The shortest bonds are the pair of parallel basal bonds, C2–C3 and C5–C6 (1.483 Å), approaching double bond length. The four equivalent bonds, attaching the apical carbon atom to the base, are long, resembling stretched single bonds (1.616 Å). The basal hydrogen atoms in **3**, like those in **1** and **21**, are bent away from the basal plane and project toward the apex.

The computed charge distribution for **3** is mostly spread over the basal carbon (34.4%) and hydrogen atoms (33.6%) with the apical carbon atom bearing a small negative charge (−0.025). Consequently, as one might expect, nucleophilic attack should take place preferentially at the basal carbon atoms of **3**. Quenching should give products of the general structure **22**, which incidentally has the same skeleton as cation **5**. Experimentally, nearly equal amounts of products substi-

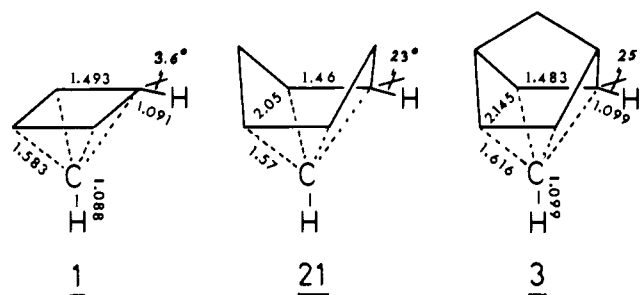
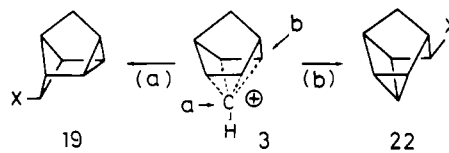


Figure 2.

tuted at the apex and base (**19** and **22**) are observed.^{8,10,17,19} Clearly, both approaches to base (b) and apex (a) are realized in practice (Scheme VIII). This apparent discrepancy could be due to microscopic reversibility. Bearing in mind that the formation of **3** from precursors of the general structure **19**

Scheme VIII



Scheme IX

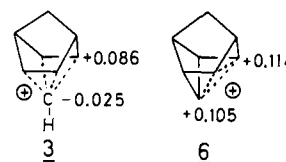


Table II. Calculated Molecular Geometries and Formal Charges of Selected C₈H₉ Cations^a



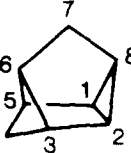
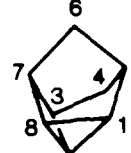

	Distances ^b in Å	Angles ^c in degrees	Formal Charges ^{b d}	
	C(1)-C(2) 1.562 C(1)-C(7) 1.554 C(2)-C(3) 1.483 C(2)-C(8) 1.616	C(1)-C(2)-C(3) 105.6 C(1)-C(2)-C(8) 93.8 C(1)-C(7)-C(4) 97.4 C(2)-C(1)-C(6) 86.8 C(2)-C(3)-C(8) 62.7 C(2)-C(1)-C(7) 104.1	C(1) 0.024 C(2) 0.086 C(7) 0.033 C(8) -0.025	H(1) 0.059 H(2) 0.084 H(7) 0.030 H(8) 0.083
3 SYMMETRICAL				
	C(1)-C(2) 1.560 C(1)-C(6) 1.559 C(1)-C(7) 1.555 C(2)-C(3) 1.481 C(2)-C(8) 1.622 C(3)-C(4) 1.566 C(3)-C(8) 1.609 C(4)-C(5) 1.566 C(4)-C(7) 1.553 C(5)-C(6) 1.482 C(5)-C(8) 1.610 C(6)-C(8) 1.624	C(1)-C(2)-C(3) 106.2 C(1)-C(2)-C(8) 94.3 C(1)-C(6)-C(5) 106.2 C(1)-C(7)-C(4) 97.3 C(2)-C(3)-C(4) 105.4 C(3)-C(4)-C(5) 87.1 C(2)-C(3)-C(8) 63.2 C(2)-C(8)-C(3) 54.6 C(2)-C(3)-C(5)-C(8) 53.0 C(3)-C(5)-C(6)-C(8) 41.6 C(2)-C(3)-C(5)-H(5) 145.4	C(1) 0.022 C(2) 0.092 C(3) 0.080 C(4) 0.027 C(5) 0.080 C(6) 0.093 C(7) 0.033 C(8) -0.026	H(1) 0.061 H(2) 0.082 H(3) 0.086 H(4) 0.058 H(5) 0.086 H(6) 0.083 H(7) 0.030 H(7') 0.030 H(8) 0.083
3 UNRESTRICTED				
	C(1)-C(2) 1.557 C(1)-C(5) 1.546 C(1)-C(8) 1.535 C(2)-C(3) 1.547 C(2)-C(8) 1.534 C(3)-C(4) 1.462 C(3)-C(6) 1.667 C(4)-C(5) 1.462 C(4)-C(6) 1.687 C(5)-C(6) 1.669 C(6)-C(7) 1.549 C(7)-C(8) 1.522	C(1)-C(2)-C(3) 102.9 C(1)-C(5)-C(4) 109.8 C(1)-C(8)-C(2) 61.0 C(2)-C(3)-C(4) 109.8 C(2)-C(3)-C(6) 97.9 C(3)-C(4)-C(5) 100.5 C(3)-C(6)-C(5) 84.7 C(3)-C(6)-C(7) 104.3 C(6)-C(7)-C(8) 100.3 C(1)-C(5)-C(3)-C(4) 145.0 C(6)-C(5)-C(3)-C(4) 101.4	C(1) -0.014 C(2) -0.013 C(3) 0.063 C(4) 0.191 C(5) 0.064 C(6) 0.053 C(7) 0.086 C(8) 0.023	H(1) 0.075 H(2) 0.076 H(3) 0.073 H(4) 0.073 H(5) 0.073 H(6) 0.050 H(7) 0.030 H(7') 0.030 H(8) 0.070
4				
	C(1)-C(2) 1.557 C(1)-C(5) 1.569 C(1)-C(8) 1.546 C(2)-C(3) 1.571 C(2)-C(8) 1.511 C(3)-C(4) 1.476 C(3)-C(7) 1.616 C(4)-C(5) 1.497 C(5)-C(6) 1.572 C(6)-C(7) 1.554 C(7)-C(8) 1.557	C(1)-C(2)-C(3) 100.9 C(1)-C(2)-C(8) 60.5 C(1)-C(5)-C(6) 103.2 C(1)-C(5)-C(4) 97.3 C(1)-C(8)-C(2) 61.2 C(2)-C(3)-C(4) 96.8 C(2)-C(3)-C(7) 87.5 C(3)-C(7)-C(8) 88.6 C(3)-C(4)-C(5) 105.6 C(1)-C(8)-C(3)-C(4) 24.1 C(1)-C(8)-C(3)-C(2) 61.7	C(1) -0.008 C(2) 0.027 C(3) -0.051 C(4) 0.407 C(5) -0.022 C(6) 0.045 C(7) 0.063 C(8) 0.016	H(1) 0.076 H(2) 0.076 H(3) 0.078 H(4) 0.039 H(5) 0.070 H(6) 0.015 H(6') 0.040 H(7) 0.050 H(8) 0.080
5				
	C(1)-C(2) 1.521 C(1)-C(7) 1.591 C(1)-C(8) 1.527 C(2)-C(3) 1.519 C(2)-C(4) 1.752 C(2)-C(8) 1.754 C(3)-C(4) 1.527 C(3)-C(7) 1.593 C(4)-C(5) 1.531 C(4)-C(8) 1.763 C(5)-C(6) 1.545 C(5)-C(8) 1.530 C(6)-C(7) 1.548	C(1)-C(2)-C(3) 92.9 C(1)-C(7)-C(3) 87.6 C(1)-C(7)-C(6) 105.6 C(1)-C(8)-C(5) 109.4 C(2)-C(1)-C(7) 89.9 C(2)-C(1)-C(8) 70.2 C(2)-C(1)-C(5) 109.4 C(3)-C(4)-C(5) 106.3 C(4)-C(5)-C(6) 70.4 C(4)-C(5)-C(8) 97.9	C(1) -0.013 C(2) 0.105 C(3) -0.012 C(4) 0.114 C(5) 0.002 C(6) 0.040 C(7) 0.054 C(8) 0.115	H(1) 0.096 H(2) 0.070 H(3) 0.096 H(4) 0.069 H(5) 0.080 H(6) 0.031 H(6') 0.032 H(7) 0.053 H(8) 0.069
6				

Table II. (Continued)

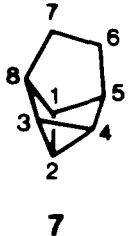
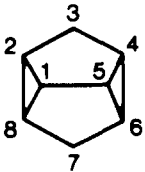
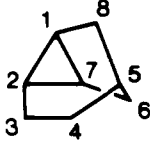
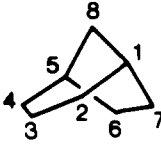
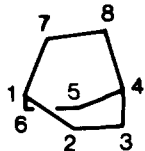
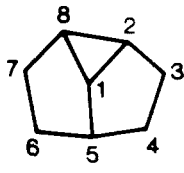
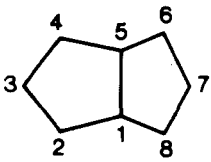
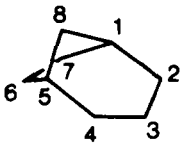
	Distances ^b in Å	Angles ^c in degrees	Formal Charges ^{b d}				
 <p>7</p>	C(1)-C(2) 1.554	C(1)-C(2)-C(3) 85.8	C(1) 0.071	H(1) 0.035			
	C(1)-C(5) 1.599	C(1)-C(2)-C(4) 85.3	C(2) 0.032	H(2) 0.084			
	C(1)-C(8) 1.585	C(1)-C(5)-C(4) 80.5	C(3) -0.004	H(3) 0.068			
	C(2)-C(3) 1.520	C(1)-C(8)-C(3) 83.2	C(4) 0.052	H(4) 0.065			
	C(2)-C(4) 1.516	C(2)-C(1)-C(8) 92.2	C(5) -0.063	H(5) 0.069			
	C(3)-C(4) 1.553	C(2)-C(3)-C(4) 58.7	C(6) 0.368	H(6) 0.039			
	C(3)-C(8) 1.557	C(2)-C(3)-C(8) 94.5	C(7) -0.046	H(7) 0.071			
	C(4)-C(5) 1.602	C(2)-C(4)-C(5) 94.8	C(8) 0.030	H(7') 0.093			
	C(5)-C(6) 1.444	C(3)-C(4)-C(5) 106.5		H(8) 0.045			
	C(6)-C(7) 1.481	C(3)-C(8)-C(7) 116.3					
	C(7)-C(8) 1.558	C(4)-C(5)-C(6) 110.4					
		C(5)-C(6)-C(7) 111.3					
		C(6)-C(7)-C(8) 103.3					
	 <p>8</p>	C(1)-C(2) 1.568	C(1)-C(2)-C(3) 106.4	C(1) 0.053	H(1) 0.068		
C(1)-C(5) 1.558		C(1)-C(2)-C(8) 56.6	C(2) -0.088	H(2) 0.083			
C(1)-C(8) 1.501		C(2)-C(1)-C(8) 62.6	C(3) 0.308	H(3) 0.055			
C(2)-C(3) 1.441		C(2)-C(3)-C(4) 112.5	C(4) -0.086	H(4) 0.082			
C(2)-C(8) 1.597		C(2)-C(1)-C(5) 105.5	C(5) 0.048	H(5) 0.067			
C(3)-C(4) 1.446		C(1)-C(8)-C(2) 60.8	C(6) 0.091	H(6) 0.060			
C(4)-C(5) 1.567			C(7) 0.016	H(7) 0.056			
C(4)-C(6) 1.591			C(8) 0.095	H(7') 0.032			
C(5)-C(6) 1.503				H(8) 0.059			
C(6)-C(7) 1.525							
C(7)-C(8) 1.527							
 <p>9</p>		C(1)-C(2) 1.480	C(1)-C(2)-C(3) 118.4	C(1) 0.106	H(1) 0.060		
		C(1)-C(7) 1.602	C(1)-C(2)-C(7) 61.8	C(2) 0.148	H(2) 0.051		
		C(1)-C(8) 1.540	C(2)-C(3)-C(4) 116.5	C(3) -0.050	H(3) 0.092		
	C(2)-C(7) 1.629	C(2)-C(7)-C(1) 54.5	C(4) 0.017	H(4) 0.079			
	C(2)-C(3) 1.503	C(3)-C(4)-C(5) 115.6	C(5) 0.025	H(5) 0.041			
	C(3)-C(4) 1.355	C(4)-C(5)-C(8) 107.3	C(6) 0.254	H(6) 0.069			
	C(4)-C(5) 1.539	C(4)-C(5)-C(6) 109.3	C(7) -0.077	H(7) 0.085			
	C(5)-C(6) 1.525	C(5)-C(6)-C(7) 109.0	C(8) 0.046	H(8) 0.032			
	C(5)-C(8) 1.566			H(8') 0.029			
	C(6)-C(7) 1.404						
	 <p>10</p>	C(1)-C(2) 1.499	C(1)-C(2)-C(3) 121.1	C(1) 0.014	H(1) 0.039		
		C(1)-C(7) 1.546	C(1)-C(8)-C(5) 99.5	C(2) 0.289	H(2) 0.043		
		C(1)-C(8) 1.564	C(1)-C(7)-C(6) 109.8	C(3) -0.136	H(3) 0.096		
		C(2)-C(3) 1.405	C(2)-C(3)-C(4) 117.4	C(4) 0.290	H(4) 0.043		
C(3)-C(4) 1.405		C(3)-C(4)-C(5) 121.0	C(5) 0.012	H(5) 0.039			
C(4)-C(5) 1.497		C(4)-C(5)-C(6) 111.5	C(6) -0.006	H(6) 0.087			
C(5)-C(6) 1.550		C(4)-C(5)-C(8) 106.8	C(7) -0.007	H(7) 0.086			
C(5)-C(8) 1.566		C(5)-C(6)-C(7) 109.5	C(8) 0.079	H(8) -0.003			
C(6)-C(7) 1.347		C(7)-C(1)-C(8) 98.5		H(8') 0.035			
		C(6)-C(5)-C(1)-C(2) 112.5					
		C(6)-C(5)-C(1)-C(8) 131.0					
 <p>11</p>		C(1)-C(2) 1.553	C(1)-C(2)-C(3) 114.8	C(1) 0.031	H(1) 0.042		
		C(1)-C(6) 1.552	C(1)-C(6)-C(5) 114.8	C(2) -0.017	H(2) 0.084		
		C(1)-C(7) 1.471	C(1)-C(7)-C(8) 117.3	C(3) -0.015	H(3) 0.085		
	C(2)-C(3) 1.353	C(2)-C(3)-C(4) 113.8	C(4) 0.086	H(4) 0.028			
	C(3)-C(4) 1.536	C(2)-C(1)-C(6) 106.9	C(5) -0.015	H(5) 0.085			
	C(4)-C(5) 1.534	C(3)-C(4)-C(5) 106.9	C(6) -0.017	H(6) 0.085			
	C(4)-C(8) 1.564	C(4)-C(8)-C(7) 107.0	C(7) 0.389	H(7) 0.037			
	C(5)-C(6) 1.353	C(4)-C(5)-C(6) 113.7	C(8) -0.050	H(8) 0.082			
	C(7)-C(8) 1.487	C(2)-C(1)-C(4)-C(5) 123.7		H(8') 0.082			
		C(3)-C(4)-C(1)-C(7) 118.6					

Table II (Continued)

	Distances ^b in Å	Angles ^c in degrees	Formal Charges ^{b d}				
 <p style="text-align: center;">12</p>	C(1)-C(2) 1.514	C(1)-C(2)-C(3) 104.9	C(1) 0.126	H(1) 0.054			
	C(1)-C(5) 1.564	C(1)-C(2)-C(8) 65.3	C(2) 0.089	H(2) 0.055			
	C(1)-C(8) 1.648	C(1)-C(8)-C(2) 56.5	C(3) -0.022	H(3) 0.085			
	C(2)-C(3) 1.512	C(2)-C(3)-C(4) 110.7	C(4) -0.011	H(4) 0.077			
	C(2)-C(8) 1.543	C(3)-C(4)-C(5) 112.3	C(5) 0.052	H(5) 0.040			
	C(3)-C(4) 1.353	C(4)-C(5)-C(1) 101.6	C(6) 0.018	H(6) 0.048			
	C(4)-C(5) 1.528	C(4)-C(5)-C(6) 115.4	C(7) 0.205	H(6') 0.048			
	C(5)-C(6) 1.540	C(5)-C(6)-C(7) 100.0	C(8) 0.019	H(7) 0.040			
	C(6)-C(7) 1.506	C(6)-C(7)-C(8) 124.8		H(8) 0.077			
	C(7)-C(8) 1.400						
 <p style="text-align: center;">13</p>	C(1)-C(2) 1.502	C(1)-C(2)-C(3) 112.0	C(1) 0.008	H(1) 0.050			
	C(1)-C(5) 1.593	C(1)-C(5)-C(4) 102.6	C(2) 0.292	H(2) 0.055			
	C(1)-C(8) 1.520	C(1)-C(8)-C(7) 111.5	C(3) -0.127	H(3) 0.105			
	C(2)-C(3) 1.399	C(2)-C(3)-C(4) 108.8	C(4) 0.297	H(4) 0.051			
	C(3)-C(4) 1.399	C(3)-C(4)-C(5) 112.9	C(5) -0.029	H(5) 0.056			
	C(4)-C(5) 1.499	C(4)-C(5)-C(6) 103.3	C(6) 0.091	H(6) 0.024			
	C(5)-C(6) 1.548	C(5)-C(6)-C(7) 104.9	C(7) 0.015	H(6') 0.003			
	C(6)-C(7) 1.506	C(6)-C(7)-C(8) 113.5	C(8) -0.024	H(7) 0.068			
	C(7)-C(8) 1.349	C(8)-C(1)-C(5)-C(4) 130.2		H(8) 0.065			
 <p style="text-align: center;">14</p>	C(1)-C(2) 1.529	C(1)-C(2)-C(3) 115.5	C(1) 0.067	H(1) 0.041			
	C(1)-C(7) 1.511	C(1)-C(8)-C(5) 111.6	C(2) 0.062	H(2) 0.028			
	C(1)-C(8) 1.546	C(1)-C(7)-C(6) 112.2	C(3) 0.019	H(2') 0.024			
	C(2)-C(3) 1.499	C(2)-C(3)-C(4) 123.8	C(4) -0.046	H(3) 0.063			
	C(3)-C(4) 1.349	C(3)-C(4)-C(5) 122.5	C(5) 0.101	H(4) 0.071			
	C(4)-C(5) 1.500	C(4)-C(5)-C(6) 125.1	C(6) 0.102	H(5) 0.041			
	C(5)-C(6) 1.512	C(5)-C(6)-C(7) 112.0	C(7) 0.104	H(6) 0.074			
	C(5)-C(8) 1.549	C(8)-C(1)-C(5)-C(6) 81.1	C(8) 0.105	H(7) 0.074			
	C(6)-C(7) 1.422	C(8)-C(1)-C(5)-C(4) 149.5		H(8) 0.071			
	C(6)-C(8) 1.688						
	C(7)-C(8) 1.690						

^a The perspective views and geometries are computer-generated from our MINDO/3 data by use of the PROJCT program.³⁰ ^b MINDO/3 values. ^c Dihedral angles are indicated by four atoms. ^d In units of the electronic charge.

(Scheme VI) requires assistance from the cyclopropane ring, then, by the same token, a nucleophile approaching **3** will pull the apical carbon atom away from the twofold molecular axis. Such an attractive distortion immediately remedies the unfavorable charge distribution as can be seen by comparing the atomic charge distribution in **3** with that of the very similar trishomocyclopropenyl cation **6** (Scheme IX).

On the other hand, more subtle effects might be operating as the proportion of attack by nucleophile at basal and apical positions depends on the degree of substitution of the delocalized framework. For example, the unbridged bishomo cation **21** is exclusively attacked at the equatorial basal position,²⁰ whereas the octamethyl derivative of **3** is quenched entirely at the apical methine position.⁹

An interesting prediction is that the small negative formal charge on the apical carbon atom of **3** will provide a sizable diamagnetic contribution to the ¹³C shielding constant. In fact, the apical ¹³C resonances of **3** and other pyramidal carbocations are all observed invariably at the highest magnetic field.^{6,8,20,26,27}

Calculation also uncovers some unexpected structural features of the apparently classical secondary cation **4** (Table II). All bond lengths are normal, except the C3-C6 and C5-C6

bonds, which are longer than the usual single bond length. Furthermore, the distance between the two formally non-bonded carbon atoms, C4 and C6, approaches single bond length and has a bicentric energy of -5.74 eV.²⁸ In corresponding fashion, the C3-C4 and C4-C5 bonds are shortened. In other words, cation **4** is a strongly delocalized species. Most (81%) of the positive charge is dispersed away from C4, much of it to C3, C5, and C7. Although no charge is transferred to the cyclopropane ring, it is interesting to note that the C1-C2 is the weakest of the cyclopropane bonds, being longer than that of cyclopropane itself (1.524 Å).²⁹ A consequence of the delocalization is the easy conversion of cation **4** to the biscyclopropylcarbanyl cation **8** (vide supra). In addition, the quenching of **4** by nucleophiles ought to give products of endo configuration, if they are formed at all.

The cation **8** (Table II) resembles a cyclopropylcarbanyl species of the bisected type.³¹ Positive charge is spread mostly between the C6 and C8 fragments. The shape of the cyclopropane ring is also affected. The bonds C2-C3 (1.441 Å) and C3-C4 (1.446 Å) connecting the two cyclopropane rings to the formal cationic center C3 are shortened, being intermediate between single and double bond in length. The distal cyclopropane bonds C1-C8 (1.501 Å) and C5-C6 (1.503 Å) are

also shortened to something less than that found in cyclopropane. However, the two side bonds of the cyclopropane ring are both lengthened, but to different degrees. The effect is comparable to that calculated for the parent cyclopropylcarbinyl cation.³²⁻³⁴

In the cation **9**, only a single cyclopropane is available to delocalize the electron deficiency, but, as the charge distribution attests, it is nonetheless nearly as efficient as both rings in cation **8**.³⁵ The repercussions on bond lengths are accordingly more pronounced. For example, the C1-C2 bond is shortened more than the comparable C1-C8 bond in **8**.

In the pair of cations **5** and **7**, the positive center is situated out of range of the cyclopropane ring, so essentially no stabilization results, as the charge distribution faithfully reflects. As expected, the shortest carbon-carbon bonds are those attached to the cationic carbon with the longest bond one removed. In cation **5**, the shortest and longest bonds are the C3-C4 and C3-C7 bonds, respectively. This hyperconjugative alternance is seen to better advantage in cation **7**, where the C1-C2 and C1-C8 bonds are more appreciably weakened and strengthened. Accentuation of these tendencies would lead in both cases to the cyclopentenyl cation **13**.

Cation **13** is far more stable than **5** or **7**, being a typical allylic species. Positive charge is largely confined to the allylic termini (C2 and C4). The carbon-carbon bond lengths of the allylic fragment are averaged (1.399 Å), becoming longer than the standard double bond length exemplified by the C7-C8 bond (1.349 Å).

Wagner-Meerwein shift of the C1-C8 bond in **13** yields **14**, of equal stability, but nonetheless a homoallylic cation. In principle, the formal positive charge on the bridge at C8 could be stabilized by interaction with either of the double bonds. However, judging from the solvolytic behavior of the *anti*-7-norbornenyl and *anti*-8-bicyclo[3.2.1]oct-2-enyl tosylates, where the former is some 10⁴ times more reactive,³⁶ charge stabilization in **14** is expected to derive from the cyclopentene part. Indeed, calculation reveals that little charge resides on C8 and that substantial transfer has occurred to C6, C7, and C5. To accommodate the charge delocalization, the C8 atom is tilted toward the C6-C7 double bond in a way reminiscent of the 7-norbornadienyl cation,³⁷ in which departure from C_{2v} symmetry is necessary for stabilization. The interatomic distances between C8, C6, and C7 are sufficiently short (1.688 Å) for sizable bonding to occur (~5.8 eV), whereas no such effect is seen between C8 and the cyclohexene moiety. By way of compensation, the C6-C7 double bond is elongated and weakened.

An interesting counterpart to the pair of cations **13** and **14**, in which the allylic-homoallylic relation is markedly different, is provided by the cations **10** and **11**. In principle, the bicyclo[3.2.1]octadienyl cation **10** should be antiaromatic²¹ if the allylic cationic and double bond fragments were able to interact through space. However, the two fragments are kept far enough apart, thereby allowing the C6-C7 double bond and the allylic fragment to display normal dimensions. The positive charge is disposed evenly on the ends of the allylic system (C2 and C4) and there is no sign of a homocyclopropenyl cation being formed by the ethylene bridge pinching the cyclohexene moiety.³⁸

The Wagner-Meerwein migration of the vinyl group in **10** to create the homoallylic cation **11**, unlike the same process for cations **13** and **14**, is energetically unfavorable. This is expected in view of the known greater thermodynamic stability of the bicyclo[3.2.1]octane over the bicyclo[2.2.2]octane skeleton.³⁹ More interestingly, it is seen that charge in **11** is not stabilized by interaction with the double bonds. Clearly, the dimensions are wrong. The distance between the cationic center at C7 and the end of the double bond (C2-C3) is just too great (2.373 Å) to permit bonding.

In summary, the ten cations may be divided into three classes. Cations **3**, **4**, and **14** are strongly delocalized species with charge being mainly spread over several carbon centers. Cations **8**, **9**, **10**, and **13** are delocalized species of the allylic and cyclopropylcarbinyl type where charge is essentially partitioned between two or three sites. Lastly, in cations **5**, **7**, and **11** the positive charge largely reposes on a single center and thus they may be considered typical classical secondary cations.

Conclusion

The present considerations cover an important segment of the C₈H₉⁺ energy surface. The MINDO/3 method, although only strictly valid for the gas phase, provides a coherent understanding of an impressive body of solution chemistry. Significant findings are the delocalization of charge where it would not be expected (cation **4**). The quantitative evaluation of charge distribution in molecules of unusual structure, such as the square pyramidal species **3**, the homoallylic (e.g., **11** vs. **14**), and the cyclopropyl species (**8**, **9** vs. **5**, **7**), provides valuable information on their chemistry. Furthermore, the establishment of the connectivity and direction of passage between these cations, in particular the concept of haptotropic displacement in the two orthogonal planes bisecting cation **3**, is not only novel, but mechanistically revealing. Lastly, our computations provide a useful guide for the planning of further experiments.

Acknowledgments. We would like to thank M. J. S. Dewar for his encouragement and for allowing us to use his program. We are also grateful for a generous allocation of computer time by the UNIVAC 1018 center of the University of Geneva. We are indebted to the Swiss National Science Foundation for the support of this research (Grant 2.2430-0.75).

References and Notes

- (1) Yoneda, S.; Yoshida, Z. *Chem. Lett.* **1972**, 607.
- (2) Kollmar, H.; Smith, H. O.; Schleyer, P. v. R. *J. Am. Chem. Soc.* **1973**, *95*, 5834.
- (3) Dewar, M. J. S.; Haddon, R. C. *J. Am. Chem. Soc.* **1973**, *95*, 5836.
- (4) Hehre, W. J.; Schleyer, P. v. R. *J. Am. Chem. Soc.* **1973**, *95*, 5837.
- (5) Stohrer, W. D.; Hoffmann, R. *J. Am. Chem. Soc.* **1972**, *94*, 1661. Williams, R. E. *Inorg. Chem.* **1971**, *10*, 210.
- (6) Hogeveen, H.; Kwant, P. W. *Acc. Chem. Res.* **1975**, *8*, 413.
- (7) Jefford, C. W.; Mareda, J.; Gehret, J. C. E.; Kabengele, nT.; Graham, W. D.; Burger, U. *J. Am. Chem. Soc.* **1976**, *98*, 2585.
- (8) Kemp-Jones, A. V.; Nakamura, N.; Masamune, S. *J. Chem. Soc., Chem. Commun.* **1974**, 109.
- (9) Hart, H.; Kuzuya, M. *J. Am. Chem. Soc.* **1974**, *96*, 6436.
- (10) Kirmse, W.; Olbricht, T. *Chem. Ber.* **1975**, *108*, 2616.
- (11) Bingham, R. C.; Dewar, M. J. S.; Lo, D. H. *J. Am. Chem. Soc.* **1975**, *97*, 1285, 1294.
- (12) Dewar, M. J. S. *Science* **1975**, *187*, 1037.
- (13) Fischer, H.; Kollmar, H. *Theor. Chim. Acta* **1970**, *16*, 163.
- (14) Dewar, M. J. S.; Lo, D. H. *J. Am. Chem. Soc.* **1971**, *93*, 7201.
- (15) Anh, N. T.; Elian, M.; Hoffmann, R. *J. Am. Chem. Soc.* **1978**, *100*, 110.
- (16) Hart, H.; Kuzuya, M. *J. Am. Chem. Soc.* **1975**, *97*, 2450, 2459. **1976**, *98*, 1545, 1551.
- (17) Coates, R. M.; Yano, K. *Tetrahedron Lett.* **1972**, 2289.
- (18) Klumpp, G. W.; Ellen, G.; Vrielink, J. J. *Tetrahedron Lett.* **1974**, 2991.
- (19) Creary, X. *J. Org. Chem.* **1975**, *40*, 3326.
- (20) Masamune, S. *Pure Appl. Chem.* **1975**, *44*, 861.
- (21) Diaz, A. F.; Sakai, M.; Winstein, S. *J. Am. Chem. Soc.* **1970**, *92*, 7477.
- (22) Cf. (a) Masamune, S.; Sakai, M.; Kemp-Jones, A. V.; Nakashima, T. *Can. J. Chem.* **1974**, *52*, 855, 858. (b) Jorgensen, W. L. *Tetrahedron Lett.* **1976**, 3029, and references cited therein.
- (23) Jefford, C. W.; Delay, A.; Genevay-Höck, S.; Mareda, J.; Burger, U. To be published.
- (24) Wiberg, K. B.; Fenoglio, R. A.; Williams, Jr., V. Z.; Ubersax, R. W. *J. Am. Chem. Soc.* **1970**, *92*, 568.
- (25) Morio, K.; Masamune, S. *Chem. Lett.* **1974**, 1107.
- (26) Coates, R. M.; Fretz, E. R. *Tetrahedron Lett.* **1977**, 1955.
- (27) Magid, R. M.; Whitehead, G. W. *Tetrahedron Lett.* **1977**, 1951.
- (28) In order to avoid overloading the present paper, we have not included the bicentric energies in the tabulation. Details are available on personal request.
- (29) "Tables of Interatomic Distances and Configurations in Molecules and Ions." *Chem. Soc., Spec. Publ.* **1958**, No. 11.
- (30) The X-Ray System, Version 1976 (XRAY 76), Stewart, J. M., Ed; Computer Science Center: University of Maryland.
- (31) Hehre, W. J. *Acc. Chem. Res.* **1975**, *8*, 369. Olah, G. A.; Spear, R. L.; Hiberty, P. C.; Hehre, W. J. *J. Am. Chem. Soc.* **1976**, *98*, 7470.
- (32) Hehre, W. J.; Hiberty, P. C. *J. Am. Chem. Soc.* **1972**, *94*, 5917.

- (33) Hoffmann, R. *Tetrahedron Lett.* **1970**, 2907. Günther, H. *ibid.* **1970**, 5173.
 (34) Dewar, M. J. S.; Haddon, R. C.; Komornicki, A.; Rzepa, H. J. *Am. Chem. Soc.* **1977**, *99*, 377.
 (35) Loew, L. M.; Wilcox, C. F. *J. Am. Chem. Soc.* **1975**, *97*, 2296.
 (36) LeBel, N. A.; Spurlock, L. A. *Tetrahedron* **1964**, *20*, 215.
 (37) Yoneda, S.; Yoshida, Z.; Winstein, S. *Tetrahedron* **1972**, *28*, 2395. Lustgarten, R. K.; Brookhart, M.; Winstein, S. *J. Am. Chem. Soc.*, **1972**, *94*, 2347.
 (38) Jefford, C. W.; Burger, U. *Chimia* **1970**, *24*, 385.
 (39) Schleyer, P. v. R.; Blanchard, K. R.; Woody, C. D. *J. Am. Chem. Soc.* **1963**, *85*, 1358.

Chemically Derivatized n-Type Silicon Photoelectrodes. Stabilization to Surface Corrosion in Aqueous Electrolyte Solutions and Mediation of Oxidation Reactions by Surface-Attached Electroactive Ferrocene Reagents

Jeffrey M. Bolts, Andrew B. Bocarsly, Michael C. Palazzotto, Erick G. Walton, Nathan S. Lewis, and Mark S. Wrighton*

Contribution from the Department of Chemistry, Massachusetts Institute of Technology, Cambridge, Massachusetts 02139. Received August 17, 1978

Abstract: Derivatization of n-type Si photoelectrode surfaces with (1,1'-ferrocenediyl)dichlorosilane results in the persistent attachment of photoelectroactive ferrocene species. Derivatized surfaces have been characterized by cyclic voltammetry in EtOH or H₂O electrolyte solutions. Such surfaces exhibit persistent oxidation and reduction waves, but the oxidation requires illumination as expected for an n-type semiconductor. The oxidation wave is observed at potentials ~300 mV more negative than at Pt, reflecting the ability to oxidize ferrocene contrathermodynamically by irradiation. Derivatized n-type Si can be used to sustain the oxidation of solution-dissolved ferrocene under conditions where "naked" Si is incapable of doing so. Further, derivatized n-type Si has been used in an aqueous electrolyte to oxidize Fe(CN)₆⁴⁻. Finally, the photooxidation of solution species has been demonstrated to occur via photogeneration of holes in the Si, oxidation of the surface-attached species, and then oxidation of the solution species by the surface-attached oxidant, providing the first direct proof of mediated electron transfer for any derivatized electrode. Derivatized electrodes can be used to sustain the conversion of light to electricity but the efficiencies are low. Based on results for 632.8-nm irradiation, solar energy conversion efficiencies of ~1% can be obtained.

We describe herein proof-of-concept experiments illustrating that deleterious photoanodic decomposition of n-type Si photoelectrodes can be substantially suppressed by chemical derivatization of the surface using a hydrolytically unstable ferrocene derivative. With the knowledge that all n-type semiconducting materials are susceptible to photoanodic decomposition,^{1,2} we regard this problem as one of the real impediments to the exploitation of semiconductor/liquid junction cells in energy conversion and photoelectrosynthesis. Further, we describe results which serve to prove that oxidation reactions at the illuminated electrode interface can be mediated by the surface-attached electroactive species. By *mediated* we mean that the surface-attached electroactive molecule is first oxidized and it then oxidizes a solution species (Scheme I). Owing to the rectifying properties of a semiconductor electrode, the mediation experiments described herein are uniquely doable at the semiconductor electrodes. Our demonstration of mediated electron transfer establishes the viability of endowing photosensitive electrodes with molecular specific properties.

In an earlier communication³ we showed that (1,1'-ferrocenediyl)dichlorosilane can derivatize the surface of n-type Si. The resulting surface exhibits persistent photoelectroactivity in that the surface-attached ferrocene species can be repetitively cycled between its oxidized and reduced form by linearly sweeping the illuminated electrode cyclically between -0.6 and +0.4 vs. a saturated calomel reference electrode (SCE). Importantly, the photooxidation of the attached ferrocene species can be effected at contrathermodynamic potentials. By this we mean that the attached species can be oxidized at an electrode potential where the attached species thermody-

namically should remain in the reduced form (vide infra). This fact, along with the relatively durable surface, reveals that it should be possible to oxidize certain solution species at contrathermodynamic potentials. In particular, any solution reductant which is oxidizable with the oxidized form of the surface-attached species should be oxidizable by illumination of the derivatized electrode. Our objective is to take advantage of the light absorption and charge-separating properties of the semiconductor, while exploiting the redox properties of the surface-bound molecule. Others have attempted to exploit the light absorption properties of covalently attached dye molecules on SnO₂⁴ or adsorbed species on other photostable oxides,⁵ in order to extend the wavelength response of large band gap semiconductor photoelectrodes.

Scheme II shows the interface energetics^{6a} for an illuminated "naked" (nonderivatized) photoelectrode compared to the derivatized case where the position of the electrode potential (E_f), top of the valence band (E_{VB}), bottom of the conduction band (E_{CB}), redox level of the attached species ($E(A^+/A)$), and the solution species ($E(B^+/B)$) are given relative to a reference electrode. We assume here that the values of E_{CB} and E_{VB} remain fixed for any value of E_f and that E_{CB} and E_{VB} are the same for the naked and derivatized surface. The stimuli of light and potential in Scheme I can be specified as being light energy great enough ($\geq E_{BG}$) to excite electrons from the valence band to the conduction band, and an electrode potential more positive than E_{CB} such that there is sufficient band bending to kinetically inhibit reduction of A^+ or B^+ for E_f more negative than $E(B^+/B)$. It is photo-generated hole formation in the valence band that allows contrathermodynamic oxidations, but the band bending in-